Electronic Supplementary Material (ESI) for Nanoscale.

Electronic Supplementary Information: Fabrication and Morphology Tuning of Graphene Oxide Nanoscrolls

Carlo A. Amadei,[a‡] Itai Y. Stein,[b‡] Gregory J. Silverberg,[a] Brian L. Wardle,[c] and Chad D. Vecitis[a*]

[a] John A. Paulson School of Engineering and Applied Sciences, Harvard University, Cambridge, MA 02138, USA. Tel: +1 (617) 496-1458; E-mail: vecitis@seas.harvard.edu

[b] Department of Mechanical Engineering, Massachusetts Institute of Technology, 77 Massachusetts Ave, Cambridge, Massachusetts 02139, USA

[c] Department of Aeronautics and Astronautics, Massachusetts Institute of Technology, 77 Massachusetts Ave, Cambridge, MA 02139, USA

‡ These authors have contributed equally to this work

S1 Graphene Oxide Synthesis

As discussed in the main text, the GO solution was prepared using a modified Hummers' method[1] with additional pre-processing of the graphite powder.[2] The preoxidation of the graphite powder (5 g; d = 45 μm) was completed using sulfuric acid (30 mL; 97% H_2SO_4), phosphorus pentoxide (4.2 g; P_2O_5), and potassium persulfate (4.2 g; $K_2S_2O_8$) in a water bath at 75°C for 4.5 h. The mixture was then cooled to room temperature and diluted with 700 mL of deionized water (DI) and vacuum filtered through a poly(tetrafluoroethylene) membrane (pore size 5 μm). After pre-oxidation, the graphite was subjected to a modified Hummers' method.[1] During this process, the pre-oxidized material was suspended in H_2SO_4 (150 mL; 97%) in an ice bath for 20 min. Potassium permanganate was slowly added (15 g; $KMnO_4$) and the mixture was heated to 35°C for 2 h. Hummers' method was completed by adding 250 mL of DI water and heating the mixture to 70°C for an additional 2 h. After quenching the reaction with hydrogen peroxide (30 mL; H_2O_2) and DI water (750 mL), it was allowed to cool to room temperature. In order to quench the unreacted reagent and clean the solution, the product was then filtered through a 300 μm testing sieve, then through glass fiber and centrifuged for 2 h at 5000 RPM (Sorvall RC-5C plus). The supernatant was then washed with hydrochloric acid (400 mL, 10% HCl). The sieving, centrifugation, and washing process was then repeated using DI (two times) and ethanol (EtOH, two times). The final solution was then dispersed in 300 mL of EtOH at a concentration of ≈ 0.1 wt. %.

S2 Graphene Oxide Nanoscroll Formation

Various stages of the formation of three different graphene oxide (GO) nanoscrolls (GONS) are displayed in Fig. S1. In Fig. S1a a large portion of the GO sheet has not scrolled, indicating an early stage of GONS formation. Fig. S1b is GONS in a more advanced state, in which the majority of the GO sheet is scrolled around the main structure. Fig. S1c is near the end of the formation of GONS as characterized by an almost complete scrolling of the GO.

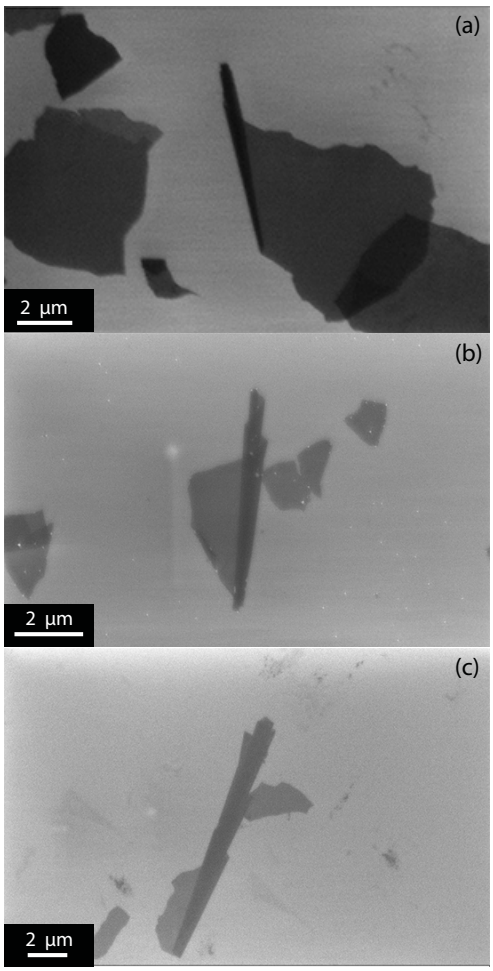

Fig. S1 Different stages of GONS formation. (a) Early stage formation. (b) Advanced stage formation. (c) Final stage formation.

The different geometries depicted in Fig. 3 in the main text can originate from the same GO flake. Fig. S2 represents a scrolled GO flake where it is possible to recognize two T-GONS and one C-GONS.

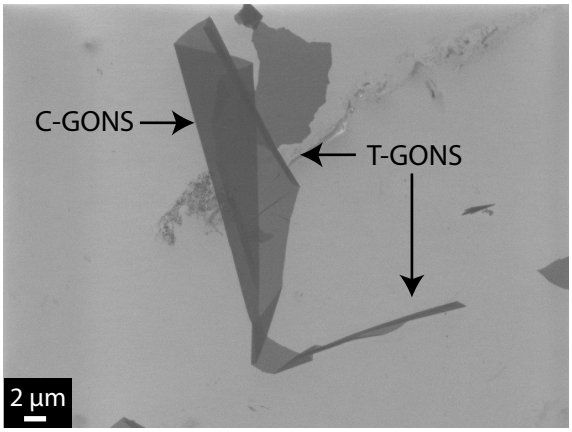

Fig. S2 Formation of a scrolled GO flake displaying simultaneously T-and C-GONS.

Fig. S3 demonstrates the hollow nature of the GONS acquired *via* transmission electron microscopy. Fig. S3a presents GONS whose tail (right side) is not scrolled in accordance with the multi-layer structure. Fig. S3b presents open-structure GONS, characteristic of an incomplete scrolling process.

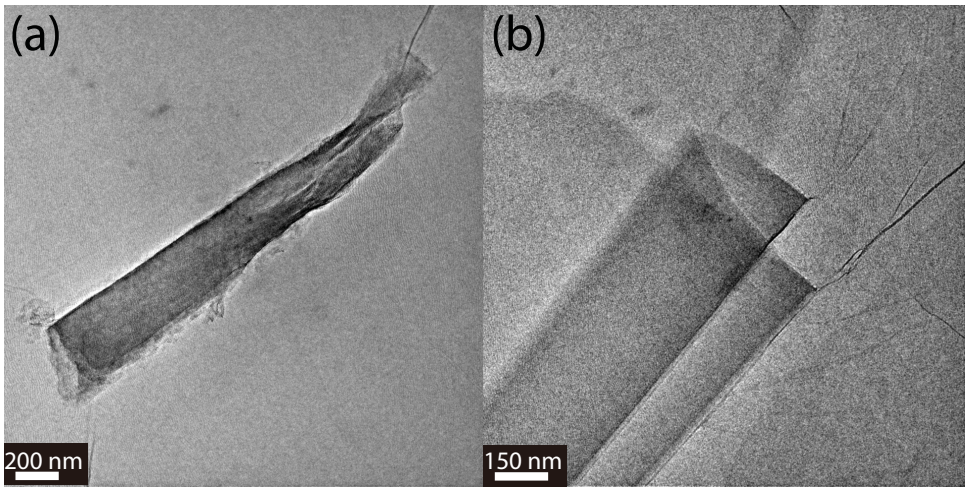

Fig. S3 Transmission electron microscopy (TEM) of GONS. (a) TEM image of GONS with a defective (wrinkled) tail. (b) TEM image of open-structure GONS formed by partial scrolling.

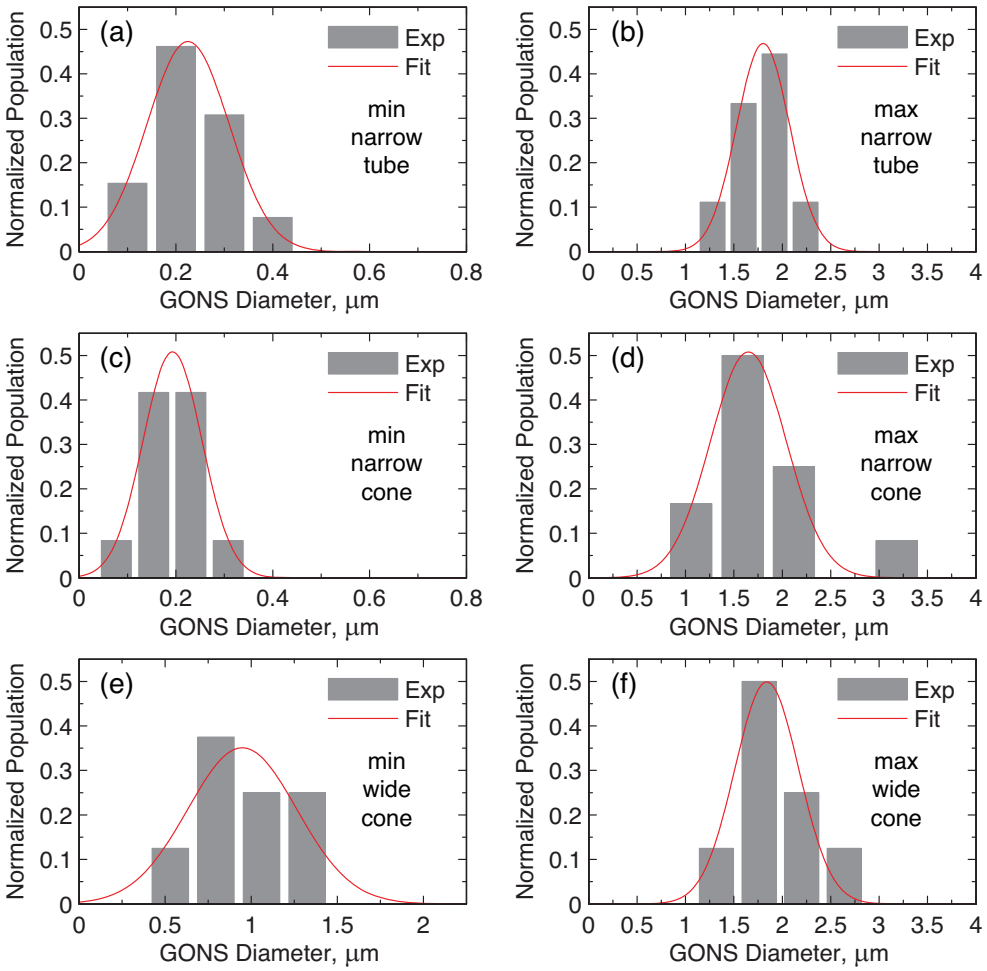

Fig. S4 Histograms of the GONS diameters and normal distribution .(a) Diameter distribution for narrow tube GONS. (b) Diameter distribution for wide tube GONS. (c) Minimum diameter distribution for narrow cone GONS. (d) Maximum diameter distribution for narrow cone GONS. (e) Minimum diameter distribution for wide cone GONS. (f) Maximum diameter distribution for wide cone GONS.

Fig. S4 represent the statistical analysis of the GONS diameters for different geometries. Statistical data is based on a population of $10-15$ GONS for each geometry. Fitting with normal distributions shows that the diameter of the narrow tube-like GONS is 225 ± 85 nm ($\mathbb{R}^2=0.9964$) while the diameter of the wide tube-like GONS is 1.802 ± 0.273 μm ($\mathbb{R}^2=0.99$). Also, the Gaussian fits show that the minimum diameters of the cone-like GONS are 193 ± 1 nm ($\mathbb{R}^2=0.9999$) for the narrow cone and 0.948 ± 0.317 μm ($\mathbb{R}^2=0.8722$) for the wide cone, while the maximum diameters are 1.65 ± 0.391 μm ($\mathbb{R}^2=0.9668$) for the narrow cone and 1.84 ± 0.331 μm ($\mathbb{R}^2=0.9548$) for the wide cone.

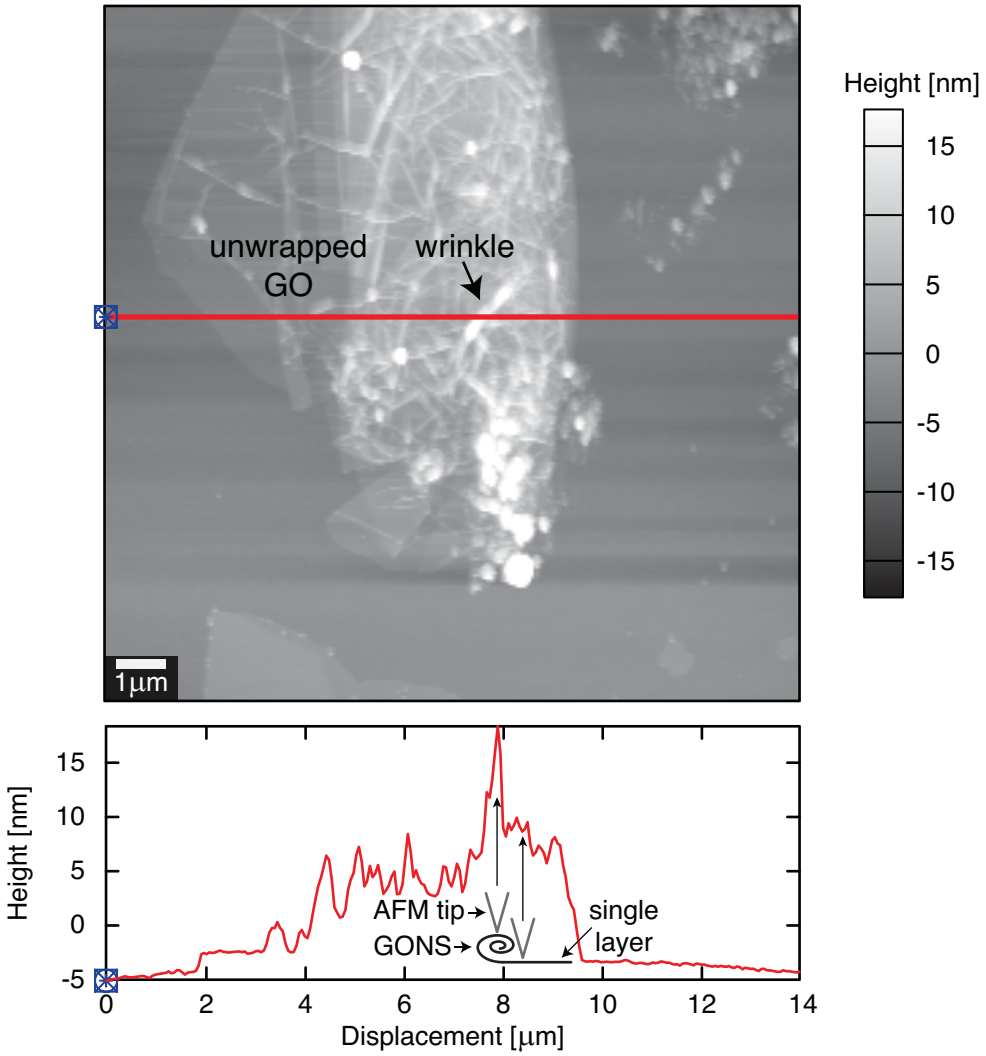

Fig. S5 AFM image of GONS and cross section line that illustrates its multilayer structure.

Fig. S5 represents an AFM image of GONS. The cross section line highlights its multilayered structure. On the left side of the image, it is possible to notice a GO flake not wrapped around the GONS characterized by a thickness of ~ 2 nm. The GONS maximum thickness is ~ 12 nm and it displays a noticeable wrinkle on the outer most layer.

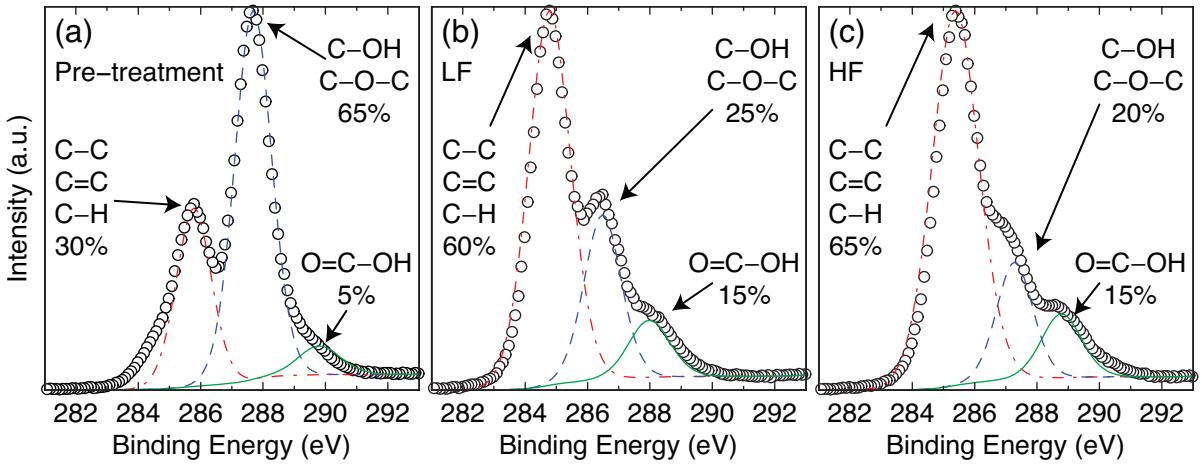

Fig. S6 XPS before and after ultrasonic treatment. (a) XPS pre-treatment. (b) XPS after 5 min ultrasonic treatment at low frequency (LF). (c) XPS after 5 min ultrasonic treatment at high frequency (HF).

Fig. S6 represents the C1s peak for the parent GO flake (Fig. S6a), after 5 minutes of LF irradiation (Fig. S6b), and 5 minutes of HF irradiation time (Fig. S6c). The post-treatment XPS shows a reduction in the C−O peak from 65% to $\approx$ 25%, and increase in C−C/C=C from 30% to $\approx$ 60% which is related to the cleavage of GO sheet at oxygen defects in the basal plane as explained in the main text.

S3 Graphene Oxide Flake and Nanoscroll Dimension Scaling

S3.1 Image Analysis

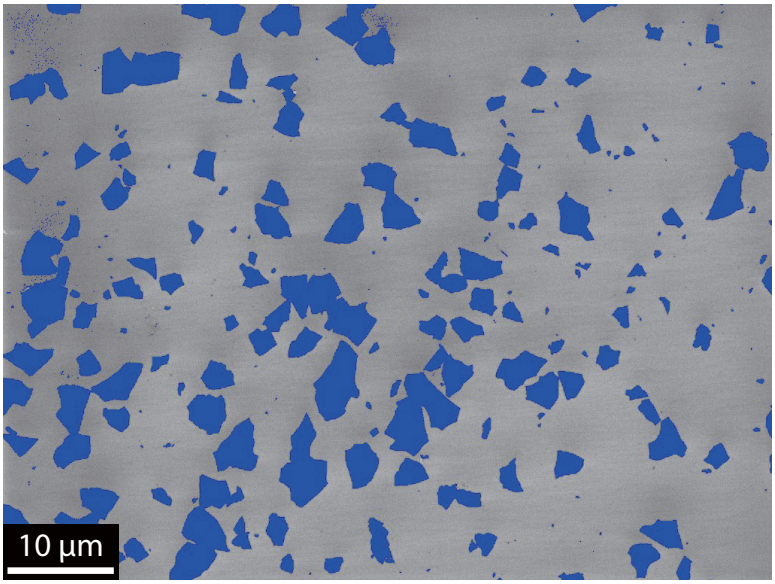

Fig. S7 Picture taken from the built-in color threshold function of ImageJ used for analyzing the GO flake area.

Fig. S7 represents an SEM image analyzed by ImageJ in order to determine the size distribution of the GO flake. The statistical analysis is based on 300 GO flakes taken from 5 different SEM images for each processing time.

S3.2 Scaling Relations

Table S1 and Table S2 present the experimental data for the GO flake area (A_{GO}) and the length of the produced GONS (L_{GONS}). See Fig. 4 and Fig. 5 in the main text for plots.

Table S1 Experimental data for the evolution of the GO flake area (A_{GO}) as a function of the treatment time (t) for both the low frequency (LF) and high frequency (HF) treatments. The values reported are the mean values and their standard errors.

t [min]	HF(1 W) A_{GO} [μm^2]	HF(10 W) A_{GO} [μm^2]	HF(20 W) A_{GO} [μm^2]	LF(10 W) A_{GO} [μm^2]	LF(100 W) A_{GO} [μm^2]
0	52.8 ± 3.9	52.8 ± 3.9	52.8 ± 3.9	52.8 ± 3.9	52.8 ± 3.9
5	53.4 ± 6.4	44.4 ± 4.9	45.5 ± 1.8	17.3 ± 1.1	3.7 ± 0.1
10	51.0 ± 4.5	39.5 ± 3.0	25.7 ± 1.5	9.8 ± 1.0	3.5 ± 0.4
20	57.1 ± 5.9	30.8 ± 2.4	13.3 ± 1.2	10.6 ± 0.7	2.7 ± 0.2
30	47.5 ± 5.2	26.0 ± 1.5	16.1 ± 1.1	8.1 ± 0.7	2.0 ± 0.2
60	51.3 ± 4.2	31.9 ± 1.7	14.6 ± 0.9	6.7 ± 0.7	1.7 ± 0.2

Table S2 Experimental data for the evolution of the graphene oxide nanoscrolls (GONS) length (L_{GONS}) as a function of the treatment time (t) for both the low frequency (LF) and high frequency (HF) treatments. The values reported are the mean values and their standard errors.

t [min]	HF(1 W) L_{GONS} [μm]	HF(10 W) L_{GONS} [μm]	HF(20 W) L_{GONS} [μm]	LF(10 W) L_{GONS} [μm]	LF(100 W) L_{GONS} [μm]
5	10.3 ± 1.2	11.3 ± 1.2	10.9 ± 1.8	6.8 ± 0.8	2.5 ± 0.4
10	9.2 ± 0.8	8.3 ± 0.8	8.2 ± 1.5	5.7 ± 0.6	2.3 ± 0.4
20	8.7 ± 1.0	6.5 ± 0.5	7.2 ± 1.2	5.4 ± 0.5	1.4 ± 0.2
30	9.0 ± 0.8	6.5 ± 0.6	7.2 ± 1.1	3.8 ± 0.6	1.0 ± 0.1
60	10.0 ± 1.0	6.8 ± 0.6	7.2 ± 0.9	2.8 ± 0.2	1.0 ± 0.1

S3.3 Solution Volume Dependence

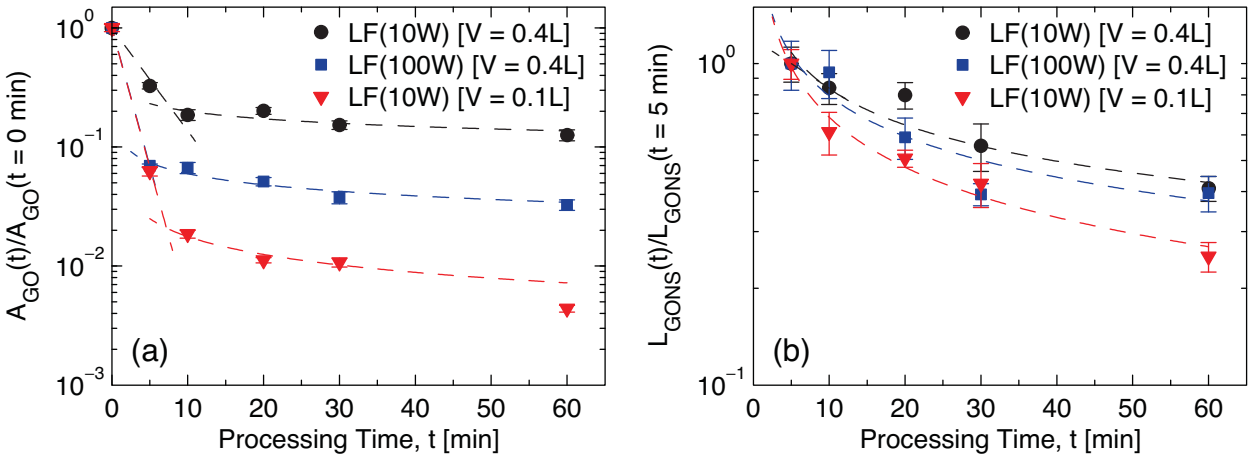

Fig. S8 Influence of the solution volume (V) on the evolution of A_{GO} and L_{GONS} as a function of the treatment time (t).

Since the volume of the GO solution used during HF and LF processing could affect the A_{GO} and L_{GONS}, but this effect will be more pronounced in the highly destructive LF treatment method, and may alter the A_{GO} and L_{GONS} evolution kinetics presented in Eq. 1 and Eq. 2 in the main text. As Fig. S8 illustrates, reducing the volume of the solution used in the LF(10W) treatment leads to a faster reduction in A_{GO} ($A_1 = 101.7\ \mu m^2$, $k_{GO} = 0.538$, $A_2 = 5.99\ \mu m^2$, $s_1 = 0.50$, and $t_{crit} = 7.1$ min) and L_{GONS} ($L_2 = 5.1\ \mu m$, $s_2 = 0.518$, and $t_{crit} \leq 5$ min), but the general kinetics are very similar to the ones observed for LF(100W) and are consistent with Eq. 1 and Eq. 2 in the main text.

References

[1] W. S. Hummers and R. E. Offeman, J. Am. Chem. Soc. **80**, 1339 (1958).

[2] N. I. Kovtyukhova, P. J. Ollivier, B. R. Martin, T. E. Mallouk, S. A. Chizhik, E. V. Buzaneva, and A. D. Gorchinskiy, Chem. Mater. **11**, 771 (1999).